HHS Public Access

Author manuscript

Exp Eye Res. Author manuscript; available in PMC 2023 May 01.

Published in final edited form as:

Exp Eye Res. 2022 May ; 218: 108988. doi:10.1016/j.exer.2022.108988.

Minimal effect of conditional ferroportin KO in the neural retina implicates ferrous iron in retinal iron overload and degeneration

Yingrui Liu[a,b], **Bailey Baumann**[b], **Ying Song**[b], **Kevin Zhang**[b], **Jacob K. Sterling**[b], **Samira Lakhal-Littleton**[c], **Zbynek Kozmik**[d], **Guanfang Su**[a,*], **Joshua L. Dunaief**[b,*]

[a]Department of Ophthalmology, The Second Hospital of Jilin University, No. 218 Ziqiang Street, Changchun, Jilin, China

[b]F.M. Kirby Center for Molecular Ophthalmology, Scheie Eye Institute, Perelman School of Medicine at the University of Pennsylvania, 305 Stellar-Chance Laboratory, 422 Curie Blvd, Philadelphia, PA, USA

[c]Department of Physiology, Anatomy and Genetics, University of Oxford, Oxford, United Kingdom.

[d]Institute of Molecular Genetics, Academy of Sciences of the Czech Republic, Academy of Sciences of the Czech Republic (ASCR), Prague, Czech Republic.

Abstract

Iron-induced oxidative stress can cause or exacerbate retinal degenerative diseases. Retinal iron overload has been reported in several mouse disease models with systemic or neural retina-specific knockout (KO) of homologous ferroxidases ceruloplasmin (*Cp*) and hephaestin (*Heph*). Cp and Heph can potentiate ferroportin (Fpn) mediated cellular iron export. Here, we used retina-specific *Fpn* KO mice to test the hypothesis that retinal iron overload in *Cp/Heph* DKO mice is caused by impaired iron export from neurons and glia. Surprisingly, there was no indication of retinal iron overload in retina-specific *Fpn* KO mice: the mRNA levels of transferrin receptor in the retina were not altered at 7–10-months age. Consistent with this, levels and localization of ferritin light chain were unchanged. To "stress the system", we injected iron intraperitoneally into *Fpn* KO mice with or without *Cp* KO. Only mice with both retina-specific *Fpn* KO and *Cp* KO had modestly elevated retinal iron levels. These results suggest that impaired iron export through Fpn is not sufficient to explain the retinal iron overload in *Cp/Heph* DKO mice. An increase in the levels of retinal ferrous iron caused by the absence of these ferroxidases, followed by uptake into cells by ferrous iron importers, is most likely necessary.

[*]Co-correspondence authors: Correspondence to: **Joshua L. Dunaief**, F.M. Kirby Center for Molecular Ophthalmology, Scheie Eye Institute, Perelman School of Medicine at the University of Pennsylvania, 305 Stellar-Chance Laboratory, 422 Curie Blvd, Philadelphia, PA 19104, USA. Tel: +1 215 898 5235, jdunaief@upenn.edu, **Guanfang Su**, Department of Ophthalmology, The Second Hospital of Jilin University, No. 218 Ziqiang Street, Changchun, Jilin, 130041, China. Tel: +86 13843091955, sugf2012@163.com.

Contributions: BB, YL, YS performed experiments. BB, YL, JLD analyzed data. YL drafted, JLD and GS reviewed and edited. All authors provided critical review of the manuscript.

Conflict of Interest: The authors declare no conflict of interest.

Keywords

retina; iron; ferrous; ferroportin; ceruloplasmin; age-related macular degeneration

Iron is critical for basic biochemical processes and metabolic pathways. Yet, excess ferrous iron can facilitate the production of hydroxyl radicals via the Fenton reaction, resulting in oxidative injury (Beard, 2001). Iron overload has been reported in neurodegenerative diseases, including age-related macular degeneration (AMD) (Dunaief, 2006), and ocular siderosis resulting from an intraocular foreign body (Burch and Albert, 1977). The retina is the most metabolically active tissue, which, along with high oxygen levels, continuous light exposure, and high levels of polyunsaturated fatty acids, makes it susceptible to oxidative stress. Thus, tight iron regulation is essential for proper cellular function.

Ferroportin (Fpn) is the only known cellular iron exporter, localizing to the plasma membrane (Donovan et al., 2005; Nemeth et al., 2004). We previously determined Fpn localization within mouse retina to: the abluminal membrane of retinal vascular endothelial cells (rVECs), the Müller glia cells, photoreceptors, and the basolateral membrane of the retinal pigment epithelium (RPE) (Theurl et al., 2016). The rVEC-specific deletion of *Fpn* resulted in iron overload in the rVECs and iron deficiency in retinal neurons and glia, indicating that iron was exported through Fpn on the abluminal side of the rVECs to enter the neural retina (Baumann et al., 2019). The homologous ferroxidases, ceruloplasmin (Cp) and hephaestin (Heph), potentiate Fpn-mediated iron export, by oxidizing iron from its ferrous (Fe^{2+}) to its ferric (Fe^{3+}) form (De Domenico et al., 2007). Only the ferric form can bind the extracellular iron carrier protein transferrin. The loss the Cp and Heph in *Cp/Heph* DKO mice resulted in age-dependent retinal iron overload by 6mo, and retinal degenerative features similar to AMD by 9mo (Hahn et al., 2004). Recently, we found that mice with *Cp* KO plus neural-retinal specific *Heph* KO generated using mRx-Cre mice (Klimova et al., 2013) also have neural retinal iron accumulation by 6mo (Baumann, Zhang et al, submitted). Impairment of ferroxidase-facilitated, Fpn-mediated iron export from retinal neurons and glia might account for these results.

The methods used to test this hypothesis are as follows. Neural retina-specific *Fpn* KO mice were generated using a strain carrying a *Fpn* floxed allele ($Fpn^{Flox/Flox}$), which was developed as described previously (Lakhal-Littleton et al., 2015). To generate conditional neural retinal KO mice, we crossed the $Fpn^{Flox/Flox}$ mice with the mRx-Cre mice. The expression of Cre within the retina in mRx-Cre+ mice was confirmed with a mouse line containing a Cre-activated GFP reporter and found to include all retinal cells except VECs and microglia (Baumann and Zhang, submitted). Mice with systemic *Cp* KO were generated as previously described (Harris et al., 1999). Mice with neural retina-specific *Fpn* KO and systemic *Cp* KO were generated by crossing the mRx-Cre+ mice to the $Fpn^{Flox/Flox}$ mice and $Cp^{-/-}$ mice. All mice were on the C57BL/6J background, and the absence of the *rd1* and *rd8* alleles was confirmed. Mice of both genders were studied. Previous studies used IP iron injection (ferric hydroxide dextran complex) to increase the serum iron levels (Moon et al., 2011), and investigate iron overload induced pathologies in the other organs (Piloni et al., 2013; Shu et al., 2019). Mice were given IP iron injections (100mg) (No. D8517,

Sigma-Aldrich, St. Louis, MO, USA) on day 1 and day 4, then euthanized on day 7. All protocols were approved by the University of Pennsylvania Institutional Review Board. All animal procedures conducted in this study were in accordance with the ARVO Statement for the Use of Animals in Ophthalmic and Vision Research. All mice were maintained in the animal facility with controlled room temperature (21–23 °C) and a 12h light/12h dark cycle. Mice were allowed at libitum access to water and a standard laboratory diet.

The mRNA levels in neural retinas were measured using qPCR. The neural retina dissection, RNA isolation, and cDNA synthesis have been described previously (Hadziahmetovic et al., 2011). Gene expression analysis was conducted on a commercial quantitative TaqMan real-time PCR 7500 detection system (Applied Biosystems, Darmstadt, Germany), performed with biological and technical triplicate reactions. GAPDH were used as an internal control. Probes used were transferrin receptor (*Tfrc*, Mm00441941), divalent transition metal (*Dmt1*, Mm01308330), ceruloplasmin (*Cp*, Mm00432654), and a custom probe for *Fpn* that spans exon 4–5. The sequences of the primers were: forward, 5′-CTATGGACTGGTGGTGGCAG -3′; reverse, 5′- ACTCCACACACATGGACACC -3′; and probe, 5′-AGGCTTGGCTATTTC-3′ (Applied Biosystems, Carlsbad, CA, USA). Statistical analyses were conducted using GraphPad version 5.0 (San Diego, CA, USA). One-way ANOVA were used for statistical analysis with the Tukey post hoc test for pairwise comparisons. All data are presented as mean ± SEM.

Immunostaining for ferritin light chain (Ft-L) was performed to assess the retinal iron levels. Retinal cryosections and immunostaining were prepared as described previously (Hadziahmetovic et al., 2011). Primary antibody: rabbit anti-Ft-L antibody (E17) (1/2500, M. Poli and P. Arosio, University of Brescia, Italy). Secondary antibody: Cy3-conjugated anti-rabbit IgG at 1/200. Control sections were processed identically except for the omission of anti-Ft-L primary antibody. Images from all sections were acquired with identical exposure parameters, using a fluorescent microscope and the Nikon Elements Software (Melville, NY, USA). The pixel density of Ft-L immunostaining was measured by ImageJ Software.

Results showed no iron accumulation occurred in the retinas of mice with neural retina-specific *Fpn* KO. Iron levels were assessed through quantification of mRNA levels of *Tfrc* and *Dmt1* using qPCR and immunostaining for Ft-L. *Tfrc* and *Dmt1* mRNAs are generally downregulated by increased cellular iron levels, and ferritin protein is upregulated. These have been previously validated as indicators of retinal iron levels (Rouault, 2006; Song et al., 2016). In 7–10-month-old mRx-Cre+, $Fpn^{Flox/Flox}$ mice, *Fpn* deletion was verified using qPCR. *Fpn* mRNA levels in the neural retina were markedly reduced compared to control mice (Fig.1 A). The mRNA levels of *Tfrc* and *Dmt1* showed no significant difference between retinas of mRx-Cre+; $Fpn^{Flox/Flox}$ mice and controls (Fig. 1B and C). Immunolabeling for Ft-L on cryosections from 7–10mo age mRx-Cre+ experimental and control mice showed no difference in labeling localization or pixel density (Fig.1 D and E). These data indicate that deletion of *Fpn* from retinal neurons and glia did not cause iron accumulation in these cells.

To "stress the system" we gave mice IP iron injections to increase their serum iron, and also crossed them with systemic *Cp* KO mice to increase ferrous iron levels. Because Cp is expressed in the liver and in macrophages, while its homologue Heph is expressed mainly in the gut, we anticipated that a Cp KO would have higher levels of serum ferrous iron than WT following IP iron injections. This ferrous iron might then be taken up by retinal cells and trapped there if Fpn normally serves as a "safety valve" to release excess iron from retinal cells. We compared iron levels in neural retinas of mice of the following genotypes given IP iron injections: neural-retina specific *Fpn* KO (mRx-Cre+, $Cp^{+/+}$, $Fpn^{Flox/Flox}$), systemic *Cp* KO (mRx-Cre+, $Cp^{-/-}$, $Fpn^{+/+}$), neural retina-specific *Fpn* KO with systemic *Cp* KO (mRx-Cre+, $Cp^{-/-}$, $Fpn^{Flox/Flox}$) and controls (mRx-Cre+, $Cp^{+/+}$, $Fpn^{+/+}$). Mice were given IP iron injections at 3mo age. One week later, mice were euthanized, and retinas were studied. To verify deletion of *Fpn* in the neural retinas of $Fpn^{Flox/Flox}$ mice and the deletion of *Cp* in $Cp^{-/-}$ mice, the mRNA levels of *Fpn* and *Cp* were measured using qPCR. As expected, the mRNA levels of *Fpn* were markedly decreased in mRx-Cre+, $Fpn^{Flox/Flox}$ mice compared to mRx-Cre+, $Fpn^{+/+}$ mice (Fig. 2A) and *Cp* mRNA was markedly decreased in the neural retinas of $Cp^{-/-}$ mice compared to $Cp^{+/+}$ mice (Fig. 2B). To evaluate the intracellular iron levels, the mRNA levels of *Tfrc* and *Dmt1* were determined using qPCR. *Tfrc* mRNA levels were modestly but significantly decreased only in mRx-Cre+, $Cp^{-/-}$, $Fpn^{Flox/Flox}$ mice compared to controls (mRx-Cre+, $Cp^{+/+}$, $Fpn^{+/+}$), indicating a small increase in iron accumulation in the neural retina of mRx-Cre+, $Cp^{-/-}$, $Fpn^{Flox/Flox}$ mice (Fig.2 C). The mRNA levels of *Dmt1* showed no difference (Fig.2 D). Immunolabelling for Ft-L was localized to retinal and choroidal vessel in all four genotypes, as expected following IP iron dextran injection (Shu et al., 2019), but there was no difference in Ft-L immunolabelling localization (Fig.2 E), or pixel density (Fig.2 F) compared to controls.

Taken together, these results are very different from those obtained in 6mo systemic *Cp/Heph* DKO mice, as well as $Cp^{-/-}$ mice with neural retinal-specific *Heph* KO, which have markedly increased levels of L-Ft immunolabeling in the neural retina indicating elevated intracellular iron levels. Since ferroxidases Cp and Heph can facilitate cellular iron export through Fpn, we tested the hypothesis that the neural retinal iron accumulation caused by Cp and Heph deficiency resulted from diminished iron export through Fpn. Surprisingly, we found that 7–10mo retina-specific *Fpn* KO mice did not have an increase in retinal Ft-L immunolabeling, nor a decrease in *Tfrc* mRNA, suggesting that impaired iron export through Fpn is not the sole mechanism of neural retinal iron overload in *Cp/Heph* DKO mice.

Since Cp and Heph are ferroxidases, their absence can lead to elevated levels of ferrous vs ferric iron in the serum and retina. The retina is predisposed to contain ferrous iron because the concentration of iron-reducing ascorbate is 1mM in the eye, which is 20 times higher than that in serum (Pirie, 1965). Unlike ferric iron, ferrous iron may be able to enter retinal cells in an unregulated manner. This is because ferric iron is primarily bound to the extracellular protein transferrin, whose uptake is downregulated in iron loaded cells by decreased levels of transferrin receptor on the plasma membrane. In contrast, the ferrous iron importers that are expressed in the retina, including Zip14, Zip8, and L-type calcium channels, are not necessarily down-regulated by increased intracellular iron. In fact, Zip14 can be upregulated (Sterling et al., 2017). Ferrous iron importers have been shown the

mediate iron overload in other organs: Zip14 expression in the liver is necessary for liver iron overload in a mouse model of hemochromatosis (Jenkitkasemwong et al., 2015).

Overall, the results reported herein emphasize the role of iron ferrous iron in retinal iron overload-induced degeneration. Supporting this, injection of ferrous sulfate into the vitreous causes elevated retinal iron levels indicated by significantly decreased *Tfrc* mRNA followed by rapid retinal degeneration (Shu et al., 2020). Also, preventing ferrous-iron induced oxidation of docosahexanoic acid (DHA) by adding a deuterated, oxidation resistant form of DHA to mouse chow prevents intravitreal iron-induced retinal degeneration (Liu et al, submitted). Further, cultured RPE cells accumulate more radiolabeled iron when it is presented as ferrous rather than ferric-transferrin (Sterling et al, submitted). The clinical implication of these results is that deuterated DHA, iron oxidases, inhibitors of ferrous iron importers, or iron chelators could be therapeutic in patients with retinal iron overload.

Acknowledgements

This research was funded by NIH/NEI EY015240, Research to Prevent Blindness, a grant from the China Scholarship Council (CSC, 202006170212) to support YL, the F.M. Kirby Foundation, the Paul and Evanina Bell Mackall Foundation Trust, a gift in memory of Dr. Lee F. Mauger.

References:

Baumann BH, Shu W, Song Y, Simpson EM, Lakhal-Littleton S, Dunaief JL, 2019. Ferroportin-mediated iron export from vascular endothelial cells in retina and brain. Experimental eye research 187, 107728. [PubMed: 31323276]

Beard JL, 2001. Iron biology in immune function, muscle metabolism and neuronal functioning. The Journal of nutrition 131, 568S–579S; discussion 580S. [PubMed: 11160590]

Burch PG, Albert DM, 1977. Transscleral ocular siderosis. American journal of ophthalmology 84, 90–97. [PubMed: 331964]

De Domenico I, Ward DM, di Patti MC, Jeong SY, David S, Musci G, Kaplan J, 2007. Ferroxidase activity is required for the stability of cell surface ferroportin in cells expressing GPI-ceruloplasmin. The EMBO journal 26, 2823–2831. [PubMed: 17541408]

Donovan A, Lima CA, Pinkus JL, Pinkus GS, Zon LI, Robine S, Andrews NC, 2005. The iron exporter ferroportin/Slc40a1 is essential for iron homeostasis. Cell Metabolism 1, 191–200. [PubMed: 16054062]

Dunaief JL, 2006. Iron Induced Oxidative Damage As a Potential Factor in Age-Related Macular Degeneration: The Cogan Lecture. Investigative Ophthalmology & Visual Science 47, 4660–4664. [PubMed: 17065470]

Hadziahmetovic M, Song Y, Wolkow N, Iacovelli J, Grieco S, Lee J, Lyubarsky A, Pratico D, Connelly J, Spino M, Harris ZL, Dunaief JL, 2011. The oral iron chelator deferiprone protects against iron overload-induced retinal degeneration. Investigative ophthalmology & visual science 52, 959–968. [PubMed: 21051716]

Hahn P, Qian Y, Dentchev T, Chen L, Beard J, Harris ZL, Dunaief JL, 2004. Disruption of ceruloplasmin and hephaestin in mice causes retinal iron overload and retinal degeneration with features of age-related macular degeneration. Proc Natl Acad Sci U S A 101, 13850–13855. [PubMed: 15365174]

Harris ZL, Durley AP, Man TK, Gitlin JD, 1999. Targeted gene disruption reveals an essential role for ceruloplasmin in cellular iron efflux. Proc Natl Acad Sci U S A 96, 10812–10817. [PubMed: 10485908]

Jenkitkasemwong S, Wang CY, Coffey R, Zhang W, Chan A, Biel T, Kim JS, Hojyo S, Fukada T, Knutson MD, 2015. SLC39A14 Is Required for the Development of Hepatocellular Iron Overload in Murine Models of Hereditary Hemochromatosis. Cell Metab 22, 138–150. [PubMed: 26028554]

Klimova L, Lachova J, Machon O, Sedlacek R, Kozmik Z, 2013. Generation of mRx-Cre transgenic mouse line for efficient conditional gene deletion in early retinal progenitors. PLoS One 8, e63029–e63029. [PubMed: 23667567]

Lakhal-Littleton S, Wolna M, Carr CA, Miller JJ, Christian HC, Ball V, Santos A, Diaz R, Biggs D, Stillion R, Holdship P, Larner F, Tyler DJ, Clarke K, Davies B, Robbins PA, 2015. Cardiac ferroportin regulates cellular iron homeostasis and is important for cardiac function. Proc Natl Acad Sci U S A 112, 3164–3169. [PubMed: 25713362]

Moon SN, Han JW, Hwang HS, Kim MJ, Lee SJ, Lee JY, Oh CK, Jeong DC, 2011. Establishment of secondary iron overloaded mouse model: evaluation of cardiac function and analysis according to iron concentration. Pediatr Cardiol 32, 947–952. [PubMed: 21656238]

Nemeth E, Tuttle MS, Powelson J, Vaughn MB, Donovan A, Ward DM, Ganz T, Kaplan J, 2004. Hepcidin regulates cellular iron efflux by binding to ferroportin and inducing its internalization. Science (New York, N.Y.) 306, 2090–2093.

Piloni NE, Fermandez V, Videla LA, Puntarulo S, 2013. Acute iron overload and oxidative stress in brain. Toxicology 314, 174–182. [PubMed: 24120471]

Pirie A, 1965. A light-calalysed reaction in the aqueous humor of the eye. Nature 205, 500–501. [PubMed: 14265299]

Rouault TA, 2006. The role of iron regulatory proteins in mammalian iron homeostasis and disease. Nature chemical biology 2, 406–414. [PubMed: 16850017]

Shu W, Baumann BH, Song Y, Liu Y, Wu X, Dunaief JL, 2019. Iron Accumulates in Retinal Vascular Endothelial Cells But Has Minimal Retinal Penetration After IP Iron Dextran Injection in Mice. Invest Ophthalmol Vis Sci 60, 4378–4387. [PubMed: 31634395]

Shu W, Baumann BH, Song Y, Liu Y, Wu X, Dunaief JL, 2020. Ferrous but not ferric iron sulfate kills photoreceptors and induces photoreceptor-dependent RPE autofluorescence. Redox biology 34, 101469. [PubMed: 32362442]

Song D, Kanu LN, Li Y, Kelly KL, Bhuyan RK, Aleman T, Morgan JI, Dunaief JL, 2016. AMD-like retinopathy associated with intravenous iron. Experimental eye research 151, 122–133. [PubMed: 27565570]

Sterling J, Guttha S, Song Y, Song D, Hadziahmetovic M, Dunaief JL, 2017. Iron importers Zip8 and Zip14 are expressed in retina and regulated by retinal iron levels. Experimental eye research 155, 15–23. [PubMed: 28057442]

Theurl M, Song D, Clark E, Sterling J, Grieco S, Altamura S, Galy B, Hentze M, Muckenthaler MU, Dunaief JL, 2016. Mice with hepcidin-resistant ferroportin accumulate iron in the retina. FASEB journal : official publication of the Federation of American Societies for Experimental Biology 30, 813–823. [PubMed: 26506980]

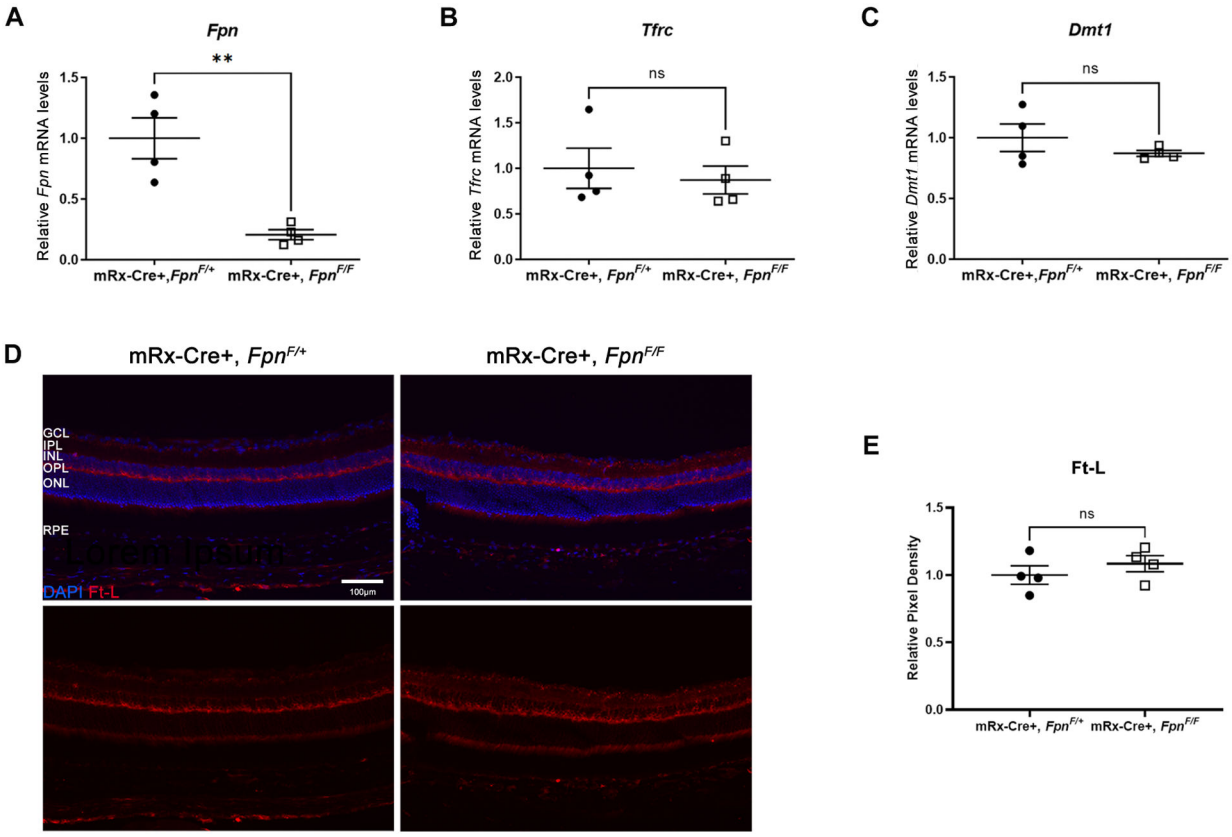

Fig. 1.

No retinal iron accumulation in neural retina-specific *Fpn* KO mice at 7–10-months of age. Graphs showing relative mRNA levels of *Fpn* (**A**), *Tfrc* (**B**), and *Dmt1* (**C**) measured by qPCR on neural retinas from neural retina-specific *Fpn* KO mice (mRx-Cre+, $Fpn^{Flox/Flox}$) versus controls (mRx-Cre+, $Fpn^{F/+}$). Representative photomicrographs showing immunolabeling for Ft-L on cryosections from mRx-Cre+, $Fpn^{Flox/Flox}$ and mRx-Cre+, $Fpn^{F/+}$ mice (**D**). Quantification of pixel density of Ft-L immunolabeling (**E**). Ganglion cell layer (GCL); inner plexiform layer (IPL); inner nuclear layer (INL); outer plexiform layer (OPL); outer nuclear layer (ONL); and retinal pigment epithelium (RPE). Scale bar: 100 µm. Error bars indicate mean ± SEM, n=4 per group. ** $P < 0.01$.

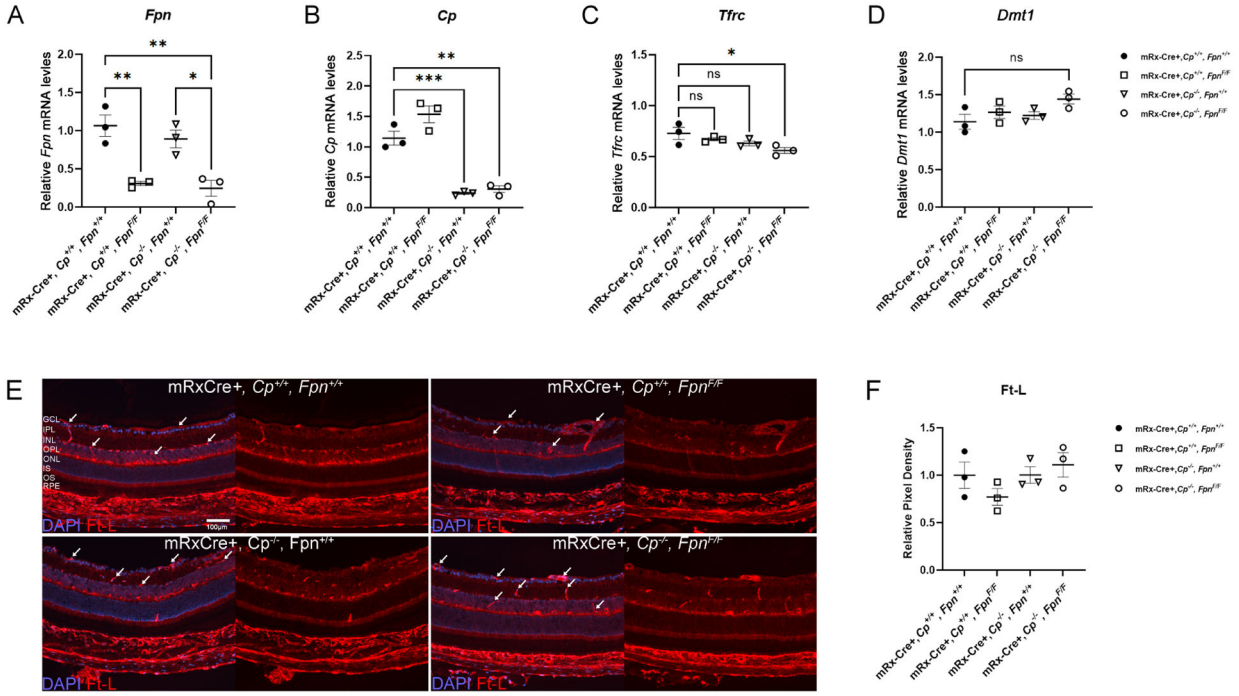

Fig. 2.

Assessment of iron accumulation in the neural retinas of neural retina-specific *Fpn* KO and/or systemic *Cp* KO mice following IP iron injection at 3mo. All mice received IP iron injections. Graphs of relative mRNA levels of *Fpn, Cp, Tfrc*, and *Dmt1* determined by qPCR in the neural retinas of mice with the indicated genotypes (**A-D**). Representative photomicrographs showing immunolabeling for Ft-L (**E**). Quantification of pixel density for Ft-L immunolabeling (**F**). Scale bar: 100 μm. Error bars indicate mean ± SEM, n=3 per group. * P <0.05, ** P < 0.01, *** P < 0.001.